Astron. Astrophys. 134, 77–86 (1984)

ASTRONOMY AND ASTROPHYSICS

Nonlinear two-dimensional dynamics of stellar atmospheres

I. A computational code

R. P. Stefanik*[,1], P. Ulmschneider[2], R. Hammer[2], and C. J. Durrant[3]

[1] Institut für Astronomie und Astrophysik, Am Hubland, D-8700 Würzburg, Federal Republic of Germany
[2] Institut für Theoretische Astrophysik, Im Neuenheimer Feld 294, D-6900 Heidelberg, Federal Republic of Germany
[3] Kiepenheuer-Institut für Sonnenphysik, Schöneckstrasse 6, D-7800 Freiburg, Federal Republic of Germany

Received February 9, accepted October 5, 1983

Summary. We present a computational code that allows the nonlinear equations of motion for a compressible fluid to be solved. Earlier work on one-dimensional problems using the method of characteristics is here generalised to two dimensions employing cylindrical geometry. The scheme is described in detail and its effectiveness is demonstrated using analytic examples of small-amplitude motion in an isothermal, stably stratified, atmosphere. The code is designed specifically to handle the problem of the overshoot and decay of convective motion in stellar atmospheres and their coupling to acoustic and internal wave fields.

Key words: convection – waves – stellar atmospheres – numerical techniques

1. Introduction

In the last decade there has been a rapidly growing awareness that stellar atmospheres are not static spherically symmetric layers characterized by just two quantities, an effective temperature and a gravitational acceleration. The current undertaking by NASA/CNRS (e.g. Jordan, 1982) to produce a series of volumes devoted to dynamical phenomena in the atmospheres of stars of all conceivable types is sufficient evidence for the importance now attached to the understanding of the non-static properties of stars. This requires first of all the identification of the modes of motion – whether wave-like or convective, for example. This may be treated in a linearized approach. But we also require a knowledge of the energetics, the excitation, damping and conversion of the various storage modes. The latter problem necessitates full non-linear treatment to describe the interplay which governs the detailed structure of stellar atmospheres.

This has long been recognized in solar physics where much attention has been given to convective motions as evidenced by the solar granulation. Of particular interest are the development and ultimate decay of these motions immediately below and within the solar photosphere whereby acoustic and gravity waves are generated (Stein, 1968; Mihalas and Toomre, 1981). These waves can propagate through the atmosphere and dissipate at higher levels. Much work has been devoted to the subject in connexion with the heating of the chromosphere, and some restricted aspects, such as the nonlinear propagation of the waves, have been thoroughly explored (Ulmschneider et al., 1978). But a fully convincing demonstration of the processes of wave generation coupled with a realistic description of the dissipation is still lacking since it requires an accurate treatment of the nonlinear dynamics in a compressible stratified medium in which most of the energy is transported by nonlocal photon exchange.

We present here a two-dimensional computational code that is designed specifically to explore such nonlinear interactions. This aim differs substantially from that of describing stellar convection per se, which has been recently reviewed by Zahn (1979). There, the main interest lies in the relationship between the superadiabatic gradient and the convective energy flux (Weiss, 1977), and, so far, all investigations resort either to the quasi-incompressible Boussinesq approximation (Spiegel and Veronis, 1960) or to the anelastic approximation (Gough, 1969). Both require that the motion does not extend vertically over too many scale heights and that the speeds developed remain small compared to the local sound speed. Acoustic waves are thereby filtered out. It is doubtful whether these conditions are met in the solar photosphere, so the fully compressible hydrodynamic equations are strictly necessary.

In Sects. 2 and 3 we present the basic equations and the numerical scheme by which they may be solved. Some test examples are given in Sect. 4 of the propagation of disturbances in a stably stratified atmosphere. Section 5 summarizes the advantages and disadvantages of this approach.

2. Basic equations

In general we are interested in unsteady, compressible flows in which there is either heat addition or heat loss by radiation from a fluid element to its surroundings. For the time being we neglect the effects of magnetic fields, viscous dissipation, and heat conduction. Since we want to model granulation flows we assume axialsymmetry where z is the vertical and r is the radial space coordinate. In cylindrical coordinates the equation expressing the conservation of mass is

$$\frac{\partial \varrho}{\partial t}+u\frac{\partial \varrho}{\partial r}+v\frac{\partial \varrho}{\partial z}+\varrho\left[\frac{\partial u}{\partial r}+\frac{\partial v}{\partial z}+\frac{u}{r}\right]=0, \tag{1}$$

where $u(r, z, t)$ is the radial and $v(r, z, t)$ is the vertical component of the velocity, respectively, and $\varrho(r, z, t)$ is the density. For a perfect

Send offprint requests to: P. Ulmschneider
* Present address: Coll. of Basic Studies, Boston University, 871 Commonwealth Ave., Boston, MA 02215, USA

gas, we have the thermodynamic relation

$$dS = c_v d\ln p - c_p d\ln \varrho , \tag{2}$$

where c_v and c_p are the specific heats, $S(r, z, t)$ is the specific entropy and $p(r, z, t)$ is the gas pressure. For simplicity we assume that c_v and c_p are constant and given by $c_v = R/[\mu(\gamma-1)]$ and $c_p = \gamma c_v$, where $R = 8.314\text{E}7\,\text{erg K}^{-1}\,\text{mol}^{-1}$ is the universal gas constant, γ is the ratio of specific heats and μ is the mean molecular weight. We take $\mu = 1.3\,\text{g mol}^{-1}$ and $\gamma = 5/3$, appropriate for the solar photosphere.

From Eqs. (1) and (2) we obtain

$$\frac{\partial p}{\partial t} + u\frac{\partial p}{\partial r} + v\frac{\partial p}{\partial z} - \frac{\gamma p}{c_p}\frac{dS}{dt} + (\gamma p)\left[\frac{\partial u}{\partial r} + \frac{\partial v}{\partial z} + \frac{u}{r}\right] = 0 , \tag{3}$$

where $\frac{d}{dt} = \frac{\partial}{\partial t} + u\frac{\partial}{\partial r} + v\frac{\partial}{\partial z}$ is the Eulerian derivative along the particle path.

The equations of conservation for the radial and the vertical momentum are given by

$$\frac{\partial u}{\partial t} + u\frac{\partial u}{\partial r} + v\frac{\partial u}{\partial z} + \frac{1}{\varrho}\frac{\partial p}{\partial r} = 0 \tag{4}$$

and

$$\frac{\partial v}{\partial t} + u\frac{\partial v}{\partial r} + v\frac{\partial v}{\partial z} + \frac{1}{\varrho}\frac{\partial p}{\partial z} + g = 0 . \tag{5}$$

For the purpose of this work, we take a constant gravitational acceleration with $g = 2.736\text{E}4\,\text{cm s}^{-2}$ appropriate for the outer portions of the Sun.

Since radiation is the only mechanism of heat transfer the energy conservation equation becomes

$$\frac{dS}{dt} = \frac{\partial S}{\partial t} + u\frac{\partial S}{\partial r} + v\frac{\partial S}{\partial z} = \left.\frac{dS}{dt}\right|_{\text{Rad}} , \tag{6}$$

where $dS/dt|_{\text{Rad}}\,(r, z, t)$ is the radiative damping function which is discussed e.g. by Kalkofen and Ulmschneider (1977). The increase in the entropy of an element of the fluid is caused by a decrease of the radiative flux. The derivative of the radiative flux, and hence $dS/dt|_{\text{Rad}}$, is obtained from a numerical solution of the equation of radiative transfer. This will be discussed in a subsequent paper. It suffices at this point to mention that similarly as our one-dimensional method (Ulmschneider et al., 1977, 1978; Kalkofen and Ulmschneider, 1977) the present approach splits the set of equations into a hyperbolic part and a parabolic-like part. The hyperbolic part as described below is solved using the method of bicharacteristics while the parabolic-like part describing the radiative damping is solved iteratively. This approach is similar to methods used by other workers (e.g. Finkleman, 1969; Finkleman and Baron, 1970; McCormack, 1976a, b). For the present, however, $dS/dt|_{\text{Rad}}$ may be presumed equal to zero.

The equation of state

$$p = \varrho\frac{RT}{\mu} , \tag{7}$$

and Eq. (2) relate the four thermodynamic variables ϱ, p, S and temperature T. Equations (3)–(6) together with initial conditions at time t and boundary conditions form a Cauchy initial-value problem of four partial differential equations in four dependent variables (u, v and any two thermodynamic variables).

3. The hydrodynamic code

a) Evaluation of numerical methods

In general, for the solution of Eqs. (3)–(6) a numerical method is required. The two most commonly employed numerical techniques are the finite difference method (FDM) and the method of characteristics (MC), both of which have been employed rather successfully in a variety of astronomical problems. The principal advantage of the FDM is that one does not need to handle shock discontinuities explicitly. This is accomplished by introducing pseudo-viscous terms into the equations of momentum and energy (von Neumann and Richtmyer, 1950), by using specially chosen differencing schemes which effectively introduce an artifical viscosity into the flow (Lax, 1954), or by introducing artifical heat conduction terms into the energy equation (Sachdev and Prasad, 1966). The dissipative effects of these artifical terms act to irreversibly convert the kinetic energy of a shock wave into internal energy of the flow. The shock front is "smeared" out into a region of rapidly but continuously varying properties and there is no need to specify conditions at moving internal shock wave boundaries.

Artifical dissipative terms (such as pseudo-viscosity), however, represent the introduction of a special kind of error into the flow calculations. It is now recognized (Richtmyer, 1973; Moretti, 1975) that shock-fitting procedures, which are essentially the application of the method of characteristics to the shock point calculations, are a desirable alternative to pseudo-viscosity methods both for reasons of accuracy and resolution. This is particularly true in multi-dimensional problems where there is generally a loss of resolution due to the increase in coarseness of the calculation grid necessitated by increased computing time, and where intricate shock wave configurations are possible and require greater resolution for definition. Furthermore, in the presence of radiation, shock-fitting procedures greatly improve the results of FDM calculations (Falle, 1976).

From this brief discussion we see that shock-fitting is a powerful alternative to artifical viscosity in FDM calculations particularly when applied to multi-dimensional problems. Since shock-fitting is simply the application of the method of characteristics to special regions of the flow it is only a trivial extension to perform a full MC calculation for the entire flow field. Furthermore, the MC is a very accurate method (cf. Hammer and Ulmschneider, 1978), since it is based on a rigorous mathematical approach, and the mathematical properties and the numerical structure of the MC can be directly related to the physical processes occurring in the flow: the network of characteristics and the dependent quantities evaluated along this network represent a detailed accounting of the generation, propagation and interaction of disturbances that carry the information which defines the flow field. The MC, therefore, has the important advantage that shock waves as well as other flow discontinuities of lower order, such as those associated with compression and rarefaction waves, are treated naturally and explicitly. For these reasons we have chosen the method of characteristics for the numerical solution of the hydrodynamic equations. This approach is similar to that taken in our work on one-dimensional problems (Stefanik, 1973; Ulmschneider et al., 1977).

b) The method of bicharacteristics

The theory of characteristics for hyperbolic equations is described in standard references (Courant and Friedrichs, 1948; Courant

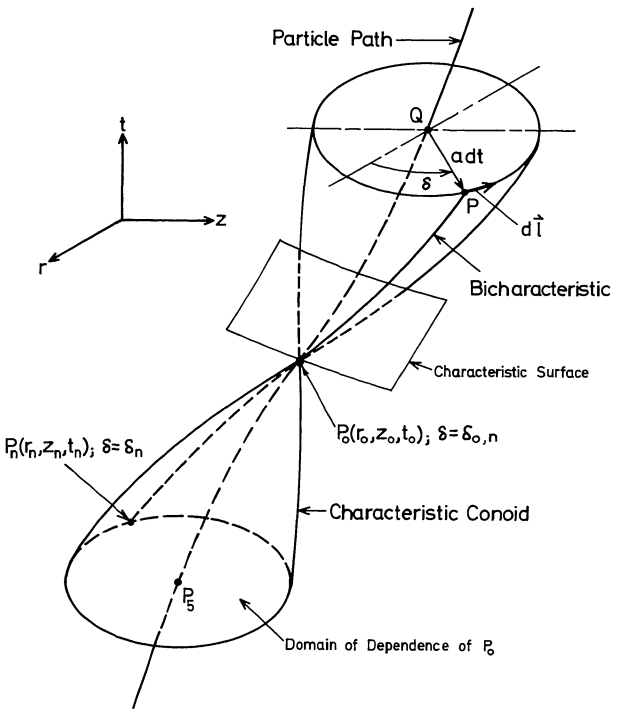

Fig. 1. Characteristic conoid in r, z, t space. The characteristic surface is tangent to the conoid along the bicharacteristic P_nP_0P

and Hilbert, 1962). For one-dimensional problems the numerical solution of a set of hyperbolic partial differential equations is well known (Lister, 1960; Hoskin, 1964; Chow, 1973; Kot, 1973; Stefanik, 1973; Ulmschneider et al., 1977). There are many applications of the method of characteristics to multi-dimensional hydrodynamic flow problems, where the method is known as the method of bicharacteristics (MBC). For our purpose interesting contributions have been made by Butler (1960), Elliot (1962), Richardson (1964), Sauerwein (1964, 1966, 1967), Strom (1965), Chu (1967), Ranson (1970), Cline and Hoffman (1972, 1973), and Shin and Valentin (1976). Equations (3)–(6) will, in general, even with smooth, analytic initial and boundary conditions, develop discontinuities in the higher-order derivatives of the dependent variables along certain surfaces, the *characteristic surfaces*, if the solution is carried beyond a certain time. In addition discontinuities of the variables themselves, that is shock waves, will develop after some time if the solution is required to be single-valued.

In multi-dimensional flows there are an infinite number of characteristic surfaces in contrast to the one-dimensional case where there are only three characteristics. The multiplicity of characteristics gives rise to many possible numerical schemes. We will use the method proposed by Butler (1960) as this method seems the most natural generalization of the one-dimensional characteristics method which we have used in our previous work (Stefanik, 1973; Ulmschneider et al., 1977).

The characteristic equations are obtained by combining the four partial differential equations (3)–(6) such that differentiation occurs only along the characteristic surfaces. The advantage of writing the hydrodynamic equations in characteristic form is that there is no differentiation across the direction of integration.

Figure 1 shows the geometry of the problem in (r, z, t)-space. The particle path or streamline characteristic and an infinite number of characteristic surfaces pass through an arbitrary point P_0. The envelope of these characteristic surfaces forms a twisted conical surface called the *characteristic conoid*. The characteristic conoid is interpreted as the surface of the space influenced by a disturbance initiated at the vertex of the conoid and whose wave front is spreading with the local sound speed a relative to the fluid. In turn, the physical state at point P_0 is influenced only by the conditions within the domain of dependence.

The tangent line of a given characteristic surface to the conoid is called a *bicharacteristic*. Bicharacteristics are interpreted as paths along which disturbances travel to P_0. A specific bicharacteristic, as seen in Fig. 1 can be identified by the angle δ (measured counter clockwise both from the positive r-axis in the upper cone and from the negative r-axis in the lower cone). The angle δ_0 at point P_0 uniquely defines the bicharacteristic. The variation of δ as a function of time is called the bicharacteristic winding. From Fig. 1 it is readily seen that the equations describing a bicharacteristic are given by

$$\left.\begin{aligned} dr &= (u + a\cos\delta)dt \\ dz &= (v + a\sin\delta)dt \end{aligned}\right\}, \tag{8}$$

Considering the line element (Fig. 1) $dl = a\,dt\,d\delta_0 = -dr/\sin\delta = dz/\cos\delta$, the requirement that bicharacteristics cannot leave the characteristic conoid is expressed by

$$-\cos\delta\frac{\partial r}{\partial\delta_0} = \sin\delta\frac{\partial z}{\partial\delta_0}, \tag{9}$$

with initial conditions

$$r = r_0, \quad z = z_0, \quad \delta = \delta_0 \quad \text{at} \quad t = t_0. \tag{10}$$

Here a, defined by

$$a^2 = \gamma\frac{p}{\varrho} = \gamma\frac{RT}{\mu}, \tag{11}$$

is the adiabatic sound velocity. For small time steps $\Delta t = t - t_0$ the bicharacteristic winding as a function of time is given by (Richardson, 1964)

$$\begin{aligned} \delta = \delta_0 + \Bigg[& \sin\delta_0\cos\delta_0\left(\frac{\partial u}{\partial r} - \frac{\partial v}{\partial z}\right) \\ & - \cos^2\delta_0\frac{\partial u}{\partial z} + \sin^2\delta_0\frac{\partial v}{\partial r} \\ & + \sin\delta_0\frac{\partial a}{\partial r} - \cos\delta_0\frac{\partial a}{\partial z}\Bigg](t - t_0). \end{aligned} \tag{12}$$

Physically, Eq. (12) describes the refraction of an acoustic ray in a medium where the propagation speed varies perpendicular to the ray direction. This can simply be derived from Snell's law.

In the method of bicharacteristics we replace the partial space-like derivatives in Eqs. (3)–(5) by derivatives along the bicharacteristic directions. The rate of change of an arbitrary function $F(r, z, t)$ along a specific bicharacteristic is then given by

$$\frac{dF}{dt} = \frac{\partial F}{\partial t} + (u + a\cos\delta)\frac{\partial F}{\partial r} + (v + a\sin\delta)\frac{\partial F}{\partial z}. \tag{13}$$

Multiplying Eq. (4) with $a\cos\delta$ and (5) with $a\sin\delta$ and adding Eqs. (3)–(5) we find, using (13),

$$dp + \varrho a\cos\delta\,du + \varrho a\sin\delta\,dv + \varrho a^2 F\,dt = 0, \tag{14}$$

where

$$F=\sin^2\delta\frac{\partial u}{\partial r}+\cos^2\delta\frac{\partial v}{\partial z}-\sin\delta\cos\delta\left(\frac{\partial u}{\partial z}+\frac{\partial v}{\partial r}\right)+\frac{u}{r}-\frac{1}{c_p}\frac{dS}{dt}\bigg|_{\mathrm{Rad}}+\frac{g\sin\delta}{a}. \tag{15}$$

In Eq. (14) the derivatives are along the direction of the bicharacteristic.

Equations (14) and (15) represent a generalization of the characteristic equations of the one-dimensional problem [Ulmschneider et al., 1977; Eqs. (15) and (17)] as can be readily seen by collapsing the r-axis and taking $\delta=\pi/2$ for the C^+ and $\delta=3\pi/2$ for the C^- characteristics. Contrary to the one-dimensional case however is the fact that in Eqs.(14) and (15) one does not succeed in replacing all space-like derivatives by derivatives along the bicharacteristic directions. These remaining space-like derivatives in Eq. (15) are an inherent complication in the two-dimensional case and prevent a straight-forward generalization of the one-dimensional method of characteristics to two dimensions.

Finally from Eq. (6) we have along the streamline characteristic

$$dS=\frac{dS}{dt}\bigg|_{\mathrm{Rad}}dt, \tag{16}$$

where for the moment we assume $\left.\frac{dS}{dt}\right|_{\mathrm{Rad}}=0$.

The streamline or particle path characteristic C^0 is defined by

$$\begin{aligned} dr&=u\,dt\\ dz&=v\,dt \end{aligned} \tag{17}$$

with initial conditions

$$r=r_0,\quad z=z_0\quad\text{at}\quad t=t_0. \tag{18}$$

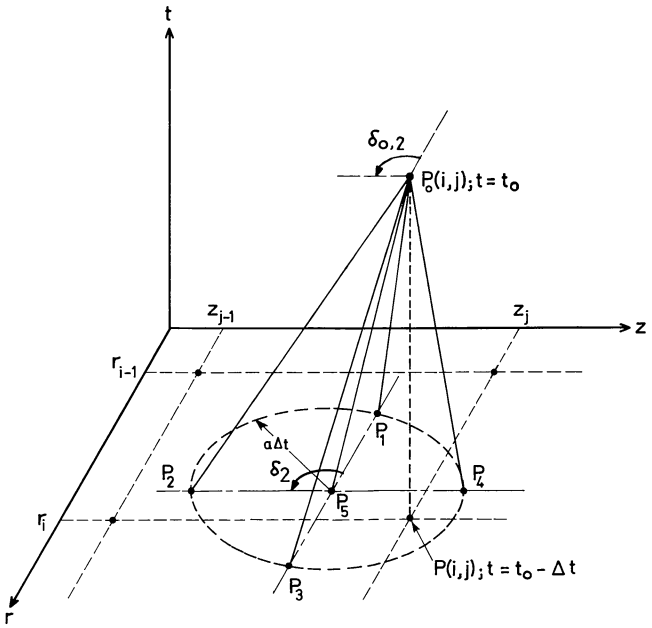

Fig. 2. Bicharacteristics geometry for the computation of the solution at grid point $P_0(i, j)$ at time t_0. In the rz plane at time $t=t_0-\Delta t$ the solution is presumed known at grid points $P(i, j)$. The bicharacteristics with $\delta_{0,n}=(n-1)\frac{\pi}{2}$, $n=1, 2, 3, 4$ intersect the rz plane at points P_n, the particle path at point P_5. Note that the angles δ_n and $\delta_{0,n}$ are measured counterclockwise from the $-r$ direction

In Fig. 2 we assume that the solution is given at time $t=t_0-\Delta t$ at the points $P(i, j)$ of the (r, z)-plane. We wish to compute the solution at the specified grid points $P_0(i, j)$ at a later time $t=t_0$. It is assumed that P_0 is sufficiently close to the (r, z)-plane that the differential Eqs. (8) and (14) to (17) may be replaced by their difference approximations. Through the point P_0 pass four bicharacteristics which intersect the (r, z)-plane at time t at points $P_n(r_n, z_n, t)$, $n=1, 2, 3, 4$. The particle path intersects at P_5. At P_0 the bicharacteristic direction is $\delta=\delta_{0,n}$ at P_n, $\delta=\delta_n$. For convenience the bicharacteristics are shown as straight lines in Fig. 2.

Along the bicharacteristic $\overline{P_0P_n}$ we write the characteristic Eqs. (14) and (15) in finite difference form by replacing other quantities by their arithmetic mean to obtain, correct to $0(\Delta t^2)$,

$$(p_0+u_0U_n+v_0V_n)-R_n=-1/2\gamma p_0F_{0,n}\Delta t, \tag{19}$$

where

$$U_n=1/2\left(\gamma\frac{p_0}{a_0}\cos\delta_{0,n}+\gamma\frac{p_n}{a_n}\cos\delta_n\right), \tag{20}$$

$$V_n=1/2\left(\gamma\frac{p_0}{a_0}\sin\delta_{0,n}+\gamma\frac{p_n}{a_n}\sin\delta_n\right), \tag{21}$$

$$R_n=p_n+u_nU_n+v_nV_n-1/2\varrho_na_n^2F_n\Delta t, \tag{22}$$

$$F_n=\sin^2\delta_n\left(\frac{\partial u}{\partial r}\right)_n+\cos^2\delta_n\left(\frac{\partial v}{\partial z}\right)_n-\sin\delta_n\cos\delta_n\left[\left(\frac{\partial u}{\partial z}\right)_n+\left(\frac{\partial v}{\partial r}\right)_n\right]+\left(\frac{u}{r}\right)_n-\frac{1}{c_p}\frac{dS}{dt}\bigg|_{\mathrm{Rad},n}+\frac{g}{a_n}\sin\delta_n, \tag{23}$$

and

$$F_{0,n}=\sin^2\delta_{0,n}\left(\frac{\partial u}{\partial r}\right)_0+\cos^2\delta_{0,n}\left(\frac{\partial v}{\partial z}\right)_0-\sin\delta_{0,n}\cos\delta_{0,n}\left[\left(\frac{\partial u}{\partial z}\right)_0+\left(\frac{\partial v}{\partial r}\right)_0\right]+\left(\frac{u}{r}\right)_0-\frac{1}{c_p}\frac{dS}{dt}\bigg|_{\mathrm{Rad},0}+\frac{g}{a_0}\sin\delta_{0,n}. \tag{24}$$

The difficulty in applying this relation is that the term $F_{0,n}$ contains the velocity derivatives $\frac{\partial u}{\partial r}$, $\frac{\partial u}{\partial z}$, $\frac{\partial v}{\partial r}$, and $\frac{\partial v}{\partial z}$ at P_0. Following Butler (1960) we eliminate these derivatives by taking the four bicharacteristics with $\delta_{0,n}=(n-1)\frac{\pi}{2}$, where $n=1$, 2, 3, and 4. From Eq. (24) we find that

$$F_{0,1}=F_{0,3}=\left(\frac{\partial v}{\partial z}\right)_0+\frac{u_0}{r_0}-\frac{1}{c_p}\frac{dS}{dt}\bigg|_{\mathrm{Rad},0}, \tag{25}$$

$$F_{0,2}=\left(\frac{\partial u}{\partial r}\right)_0+\frac{g}{a_0}+\frac{u_0}{r_0}-\frac{1}{c_p}\frac{dS}{dt}\bigg|_{\mathrm{Rad},0}, \tag{26}$$

and

$$F_{0,4}=\left(\frac{\partial u}{\partial r}\right)_0-\frac{g}{a_0}+\frac{u_0}{r_0}-\frac{1}{c_p}\frac{dS}{dt}\bigg|_{\mathrm{Rad},0}. \tag{27}$$

If we denote Eq. (19) by the symbol E_n we eliminate the unwanted derivatives by forming the linear combinations E_1-E_3 and E_2-E_4 to obtain

$$v_0=\frac{(U_1-U_3)\left(R_4-R_2+\gamma\frac{p_0}{a_0}g\Delta t\right)+(R_1-R_3)(U_2-U_4)}{(V_1-V_3)(U_2-U_4)-(U_1-U_3)(V_2-V_4)} \tag{28}$$

and

$$u_0=\frac{(R_1-R_3)-v_0(V_1-V_3)}{(U_1-U_3)}. \tag{29}$$

For the system to be complete we need two additional equations. One is obtained by forming the linear combination of Eq. (19) for $n=1, 2, 3, 4$, $\sum_{n=1}^{4} E_n$, and then subtracting from it Eq. (3), written in difference form along the streamline characteristics, to obtain equation E_5,

$$p_0=1/2\sum_{n=1}^{4}R_n-R_5-1/2\gamma p_0\left(\frac{u_0}{r_0}-\frac{1}{c_p}\frac{dS}{dt}\bigg|_{\text{Rad},0}\right)\Delta t - \frac{u_0}{2}\sum_{n=1}^{4}U_n-\frac{v_0}{2}\sum_{n=1}^{4}V_n, \tag{30}$$

where

$$R_5=p_5-1/2\gamma p_5\Delta t\left[\left(\frac{\partial u}{\partial r}\right)_5+\left(\frac{\partial v}{\partial z}\right)_5+\frac{u_5}{r_5}-\frac{1}{c_p}\frac{dS}{dt}\bigg|_{\text{Rad},5}\right]. \tag{31}$$

The final relation is obtained from Eq. (16) applied along the particle path,

$$S_0=S_5+1/2\Delta t\left[\frac{dS}{dt}\bigg|_{\text{Rad},0}+\frac{dS}{dt}\bigg|_{\text{Rad},5}\right]. \tag{32}$$

Equations (28)–(30) and (32) form a system of four equations for v_0, u_0, p_0 and S_0 in terms of conditions at P_n, $n=1, 2, 3, 4$. To these we must add expressions relating the coordinates of P_0 to those at P_n. These are obtained from the Eqs. (8) and (17) for the characteristics directions, which when written in finite difference form, correct to second order in Δt, are

$$r_n=r_0-1/2\,(u_0+u_n+a_0\cos\delta_{0,n}+a_n\cos\delta_n)\Delta t \tag{33}$$

and

$$z_n=z_0-1/2\,(v_0+v_n+a_0\sin\delta_{0,n}+a_n\sin\delta_n)\Delta t, \tag{34}$$

where $n=1, 2, 3, 4$ for the bicharacteristics and

$$r_5=r_0-1/2(u_0+u_5)\Delta t \tag{35}$$

and

$$z_5=z_0-1/2(v_0+v_5)\Delta t \tag{36}$$

for the streamline characteristics. The formulation is completed with Eq. (12) which relates δ_n at time $t=t_0-\Delta t$ with $\delta_{0,n}$ at time t_0.

The procedure to solve for the physical variables at point P_0 is as follows. With rough estimates of the physical variables at points P_n ($n=0, 1, 2, 3, 4, 5$) improved positions r_n, z_n ($n=1, 2, 3, 4, 5$) for the points P_n are calculated with Eqs. (12) and (33)–(36). With an interpolation scheme described below physical variables and their derivatives are then evaluated at the new points P_n from the known solution at the grid points $P(i,j)$. Using Eqs. (12), (20)–(23), and (28)–(32) new physical variables u_0, v_0, p_0, S_0 are then computed for point P_0 etc. This procedure, called hydrodynamic iteration, converges rapidly and eight digit accuracy is usually achieved in no more then four iterations.

c) Boundary conditions, boundary points

For the astrophysical application to granulation flows we consider a cylindrical volume where the axis of symmetry is the z-axis which points in the outward vertical direction. The cylinder is assumed to have a flat top and a flat bottom. We consider two types of boundary conditions. In case 1 the cylinder has *rigid boundaries* everywhere. That is, at the top and bottom boundaries the vertical velocity component v vanishes and at the radial cylindrical boundary the horizontal velocity u vanishes. In case 2 we have rigid boundaries everywhere except at the top where we now assume a *transmitting boundary*. This type of boundary condition has been used in our one-dimensional work (Ulmschneider et al., 1977) and has recently also been discusssed by Hedstrom (1979). For a transmitting boundary we assume that along the bicharacteristic number 2 we have

$$v_0=v_2. \tag{37}$$

We performed several tests of this transmitting boundary condition and like in our one-dimensional work found excellent transmission for sound waves.

The method of computation of boundary points is illustrated in Fig. 3. Due to the confinement of the fluid some of the bicharacteristics used for interior points are not available for the computation of boundary points. At normal boundary points (see Fig. 3) one of the four bicharacteristics is missing and at corner points two are missing. On the lower boundary for example we have $v_0=0$ from the boundary condition. Equation (29) provides u_0. The winding of bicharacteristics number 1 and 3 (see Fig. 3) is computed as for an interior point in the case where $\frac{\partial(a\pm u)}{\partial z}<0$ (+ for 1 and − for 3). In the case $\frac{\partial(a\pm u)}{\partial z}\geqq 0$ no winding occurs as here information travels along the boundary. S_0 is given by Eq. (32). The remaining unknown, p_0, is computed by forming the linear combination $E_1+E_3+2E_4-2E_5$ of the Eqs. (19) and (30).

$$p_0=1/2\left[R_1+R_3+2R_4-2R_5-u_0(U_1+U_3+2U_4)-v_0(V_1+V_3+2V_4)-\gamma p_0\Delta t\left(\frac{u_0}{r_0}-\frac{1}{c_p}\frac{dS}{dt}\bigg|_{\text{Rad},0}-\frac{g}{a_0}\right)\right]. \tag{38}$$

For case 1 the normal points on the top boundary are computed similarly as those at the bottom boundary. For case 2 the points P_1, P_3, P_5 do not necessarily lie on the boundary. Here slight extrapolations of the solution at the old time level might be necessary. This acts to restrict the time step and is discussed below. The normal points on the axis of symmetry and on the radial cylindrical boundary are computed similarly to the bottom boundary.

For the corner points the procedure likewise is straightforward. For the corner at the top boundary and the axis of symmetry in case 1, for instance, $u_0=v_0=0$ while S_0 is found from Eq. (32). p_0 is computed by forming the linear combination $E_3+E_2-E_5$ of

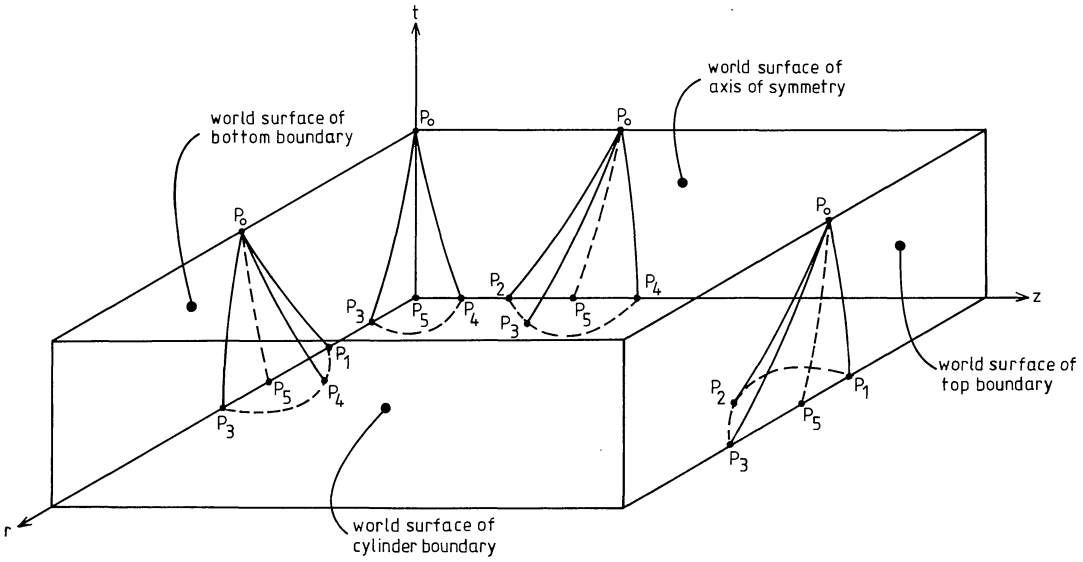

Fig. 3. Bicharacteristics at boundary points. At normal boundary points one and at corners two of the four bicharacteristics used for interior points are missing

Eqs. (19) and (30) from which one finds

$$p_0 = R_2 + R_3 - R_5 - v_0(V_2 + V_3) - \gamma p_0 \frac{\Delta t}{2}\left(\frac{u_0}{r_0} - \frac{1}{c_p}\frac{dS}{dt}\bigg|_{\mathrm{Rad},0} + \frac{g}{a_0}\right). \tag{39}$$

Note that here as well as at other points on the axis of symmetry $\frac{u_0}{r_0}$ or $\frac{u_5}{r_5}$ must be replaced by the derivatives $\frac{\partial u}{\partial r}$ as $r=0$ for these points. For the winding similar considerations exist as for the edge points.

d) Interpolation, boundary behaviour, time step

To compute the solution at grid point $P_0(i,j)$ at time $t=t_0$ the five physical variables x (u, v, p, S, dS/dt_{Rad}) have to be known at the grid points P (i,j) at time $t=t_0-\Delta t$ (see Fig. 2). As the method requires the solution and its derivatives at the foot points P_n $(n=1,\ldots,5)$ an interpolation scheme is necessary to evaluate the desired quantities from the known solution at $P(i,j)$. Such an interpolation scheme, as has been found by Hammer and Ulmschneider (1978) for one-dimensional cases, is crucial for the accuracy of the modified method of bicharacteristics. Following Hammer and Ulmschneider in order to optimize the efficiency of the code, we have chosen a two-dimensional cubic spline interpolation as described by Späth (1973). In this method, any variable x is represented by a smooth surface which for each grid cell $(r_i \leqq r < r_{i+1},\ z_j \leqq z < z_{j+1})$ is of bicubic form,

$$x(i,j;r,z) = \sum_{k,l=1}^{4} c_{ijkl}(r-r_i)^{k-1}(z-z_j)^{l-1}. \tag{40}$$

The interpolation coefficients c_{ijkl} are determined such that the resulting interpolation surface goes through the points $x_{ij}=x(r_i,z_j)$ and has two continuous derivatives. This can be done only if at the boundaries certain derivatives of the variable x are specified, namely $\partial x/\partial r$ at the axis of symmetry and at the radial cylinder boundary, $\partial x/\partial z$ at the top and bottom boundaries, and $\partial^2 x/\partial r\partial z$ at the corners. Some of these derivatives follow from symmetry and mathematical arguments, others have to be approximated numerically. At the axis of symmetry, the r derivatives of all variables, except u, must vanish, and thus the same holds for the mixed derivatives at the inner corners. This is because we do not allow a discontinuous slope of the variables v, p, S, dS/dt_{Rad} at the axis of symmetry. At the bottom boundary and also in the case of a rigid top boundary, the z-derivative of the pressure after Eq. (5) is determined by the hydrostatic equation, $\partial p/\partial z = -\varrho g$. Finally from Eq. (4) follows that at the outer boundary $\partial p/\partial r = 0$, and thus $\partial^2 p/\partial r\partial z = 0$ at the outer corners. All of the other boundary derivatives must be computed from numerical approximations. Various tests showed that for this purpose the simple one-sided difference formula was fully sufficient and led to very small interpolation errors of the variables as well as of their derivatives.

Interpolation formulae for the derivatives $\partial x/\partial r$ and $\partial x/\partial z$ follow immediately from Eq. (40). The optimal way of evaluating such formulae is the double Horner's rule. Furthermore we modified the Späth (1973) algorithm such that the four-dimensional coefficient arrays could be mapped onto one-dimensional arrays during the evaluation of these formulae, exploiting the specific way of storage of multi-dimensional arrays in the computer. This modification reduced the computer time spent for interpolation by a factor of almost 4.

4. Test calculations

a) Linearized standing wave solutions

The most stringent test of the performance of the code that we could devise was to compare its results with analytic solutions. So far as we know, these exist only in the linear regime for motions with cylindrical symmetry; the classes of exact nonlinear solutions in Cartesian geometry described by Chiu (1970) unfortunately cannot be generalized.

The linearized forms of Eqs. (1) and (4)–(7), in the case of an isothermal atmosphere with constant ratio of specific heats γ, can be combined to yield the well-known wave equation for the velocity $\boldsymbol{v}=(u,v)$

$$\frac{\partial^2 \boldsymbol{v}}{\partial t^2} = a^2 \nabla(\nabla\cdot\boldsymbol{v}) + (\gamma-1)\boldsymbol{g}(\nabla\cdot\boldsymbol{v}) + \nabla(\boldsymbol{g}\cdot\boldsymbol{v}), \tag{41}$$

whose solutions for the radial velocity are (cf. Stix, 1969)

$$u=u_0\exp(i\omega t)\exp(i\kappa z)\begin{cases}J_1(\alpha r)\\ Y_1(\alpha r)\end{cases}. \tag{42}$$

J_1 and Y_1 are Bessel functions of the first order and the frequency ω and wave numbers κ, α satisfy the dispersion relation (identical to that of the Cartesian case)

$$\omega^4-\omega^2[a^2(\kappa^2+\alpha^2)+i\kappa\gamma g]+(\gamma-1)g^2\alpha^2=0\,. \tag{43}$$

The complete progressive wave solutions are then

$$u=u_0\exp(i\omega t)\exp(\gamma gz/2a^2)\exp(ikz)\begin{cases}J_1(\alpha r)\\ Y_1(\alpha r)\end{cases}, \tag{44}$$

$$v=u_0\alpha\frac{(\gamma/2-1)g-ia^2k}{\omega^2-a^2k^2-\gamma^2g^2/4a^2}\exp(i\omega t)\exp(\gamma gz/2a^2)\cdot\exp(ikz)\begin{cases}J_0(\alpha r)\\ Y_0(\alpha r)\end{cases}, \tag{45}$$

$$p'=\frac{i\varrho_0}{\omega}\frac{\omega^2-(\gamma-1)g^2/a^2}{(\gamma/2-1)g/a^2-ik}v\,, \tag{46}$$

$$\varrho'=\frac{i\varrho_0}{\omega a^2}\frac{\omega^2-\gamma(\gamma-1)g^2/2a^2+i(\gamma-1)gk}{(\gamma/2-1)g/a^2-ik}v\,, \tag{47}$$

where the real vertical wave number $k=\kappa+i\gamma g/2a^2$ now satisfies

$$\omega^4-\omega^2[a^2(k^2+\alpha^2)+\gamma^2g^2/4a^2]+(\gamma-1)g^2\alpha^2=0\,. \tag{48}$$

For given α, k, this yields two solutions for the frequency, the higher corresponding to the acoustic mode and the lower to the internal gravity mode. Each can produce standing waves in a box with rigid reflecting boundaries. It should be noted that besides progressive waves Eq. (41) admits evanescent waves but these are not allowed in a finite slab with our boundary conditions.

The standing wave solutions are simply

$$v=Ma\sin\omega t\exp(\gamma gz/2a^2)\sin kzJ_0(\alpha r)\,, \tag{49}$$

$$u=\frac{M}{ak\alpha}\frac{\omega^2-a^2k^2-g^2\gamma^2/4a^2}{1+(\gamma/2-1)^2g^2/a^4k^2}\sin\omega t\exp(\gamma gz/2a^2)\cdot[\cos kz+(\gamma/2-1)g/a^2k\sin kz]J_1(\alpha r) \tag{50}$$

$$p'=\frac{M\varrho_0a}{\omega k}\frac{\omega^2-(\gamma-1)g^2/a^2}{1+(\gamma/2-1)^2g^2/a^4k^2}\cos\omega t\exp(\gamma gz/2a^2)\cdot[\cos kz+(\gamma/2-1)g/a^2k\sin kz]J_0(\alpha r)\,, \tag{51}$$

$$\varrho'=\frac{M\varrho_0}{k\omega a}\frac{\omega^2-(\gamma-1)g^2/a^2}{1+(\gamma/2-1)^2g^2/a^4k^2}\cos\omega t\exp(\gamma gz/2a^2)\cdot\left[\cos kz+\frac{\omega^2-(\gamma-1)a^2k^2/(\gamma/2-1)-g^2\gamma(\gamma-1)/2a^2}{\omega^2-(\gamma-1)g^2/a^2}\cdot(\gamma/2-1)\frac{g}{a^2k}\sin kz\right]J_0(\alpha r)\,, \tag{52}$$

where $\varrho_0(z)$ is the density in the undisturbed atmosphere, ϱ', p' are the first-order perturbations in density and pressure and M is the vertical Mach number evaluated at $z=0$ which we here take to be the upper boundary of the box. The boundary conditions are now fulfilled if we choose αR to be a zero of the first-order Bessel function, R being the radius of the box, and $kZ=n\pi$ where Z is the depth of the box.

We illustrate the results of the test case in which $Z=380$ km, $R=100$ km, $T=5000$ K, $\gamma=5/3$ and the pressure at the upper boundary 10^4 dyn cm^{-2}. In the undisturbed atmosphere the pressure increases 26-fold to the lower boundary. We modelled a half wave in both vertical and horizontal directions ($kZ=\pi$, $\alpha R=3.81371$) which had 20 and 6 grid points respectively, spaced 20 km apart. The dispersion relation (48) predicts the periods of the waves to be 21.95 s (acoustic) and 210.1 s (internal gravity).

The system was released from rest with the density and pressure perturbations given by Eqs. (51) and (52), setting $t=0$, and the resulting motion was followed over at least one complete cycle for Mach numbers of 0.1 and 0.01.

Despite the limited number of grid points, the use of single precision (5 significant figures on an IBM 370−168) and the neglect of winding, the numerical solution reproduced the analytical quite satisfactorily. With $M=0.01$, after 16 steps of 1.37 s each, the error in the pressure along the axis due to the acoustic waves was a maximum of 0.4% at the upper boundary and less than 0.01% below midpoint of the box, the errors being measured relative to the total pressure. This case develops a maximum temperature perturbation of 155 K and vertical and horizontal velocities of 37 m s^{-1} and 184 m s^{-1}. Since the horizontal wave number is some four times the vertical, the acoustic waves propagate almost horizontally, hence the horizontal velocities are substantially larger than the vertical. Nevertheless, the amplitudes are such that the solution remains in the linear regime. This is demonstrated in Fig. 4a, which shows the most significant thermodynamic variable, the pressure, on the central axis and on the outer boundary at $t=0$, 10.9, 21.9 and 32.9 s. At $t=0$, the values are those of the analytic solution, which are smoothly and accurately reproduced at each halfcycle (the sign of the fluctuation has been changed at each odd value for better comparison). The same is true of the vertical and horizontal velocities which are shown in Fig. 4b as a function of height at the cut where the maximum values are achieved, the axis of the cylinder and 40 km from the axis, respectively.

When the Mach number is raised to 0.1, the initial temperature perturbation reaches 30% of the temperature of the undisturbed atmosphere, and this is quite sufficient to produce nonlinear effects. Already after 11 s the smooth pressure profile on the axis shows distortion (Fig. 4a right-hand side). Before one period is complete a harmonic appears in the vertical velocity profile (Fig. 4b right-hand side).

In the case of the internal gravity wave, the motion is primarily vertical, so the relative amplitudes of the vertical and horizontal velocities are interchanged. The imposed Mach number now governs the size of the total velocity and the motion for both $M=0.1$ and $M=0.01$ remains in the linear regime. Buoyancy takes over from pressure as the major restoring force, so we show the temperature fluctuations in Fig. 5a which mirrors the almost equal and opposite relative density perturbations. The maximum values are 21 and 212 K for $M=0.1$ and 0.01. Note that the pressure distribution in the acoustic wave is dominated by the $\cos kz$ term in Eq. (51) but the temperature perturbation in the internal wave is dominated by the $\sin kz$ term. The velocity profiles, taken on the same cuts as Fig. 4b, are quite stable in both cases (Fig. 5b). The initial values are reproduced after 153 time steps with an error of temperature of 0.03% at the upper boundary and less than 0.001% in the lower half ($M=0.01$); the maximum error increases to 0.1% for $M=0.1$.

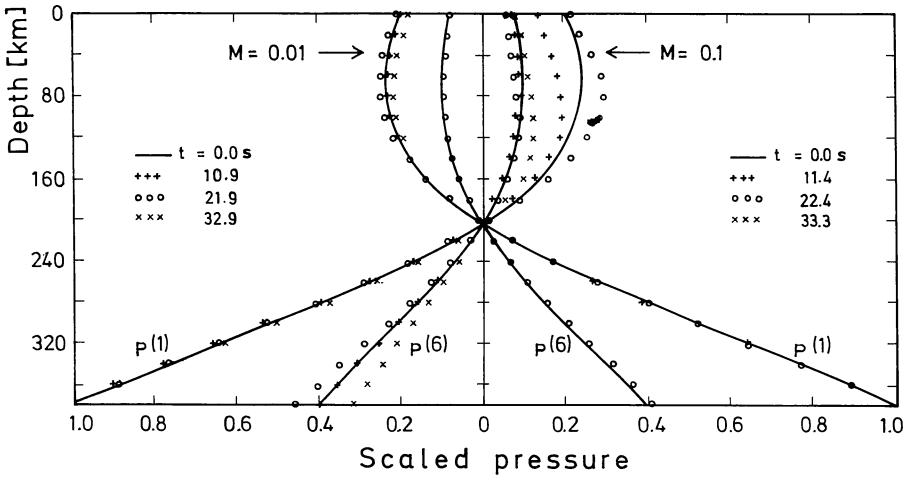

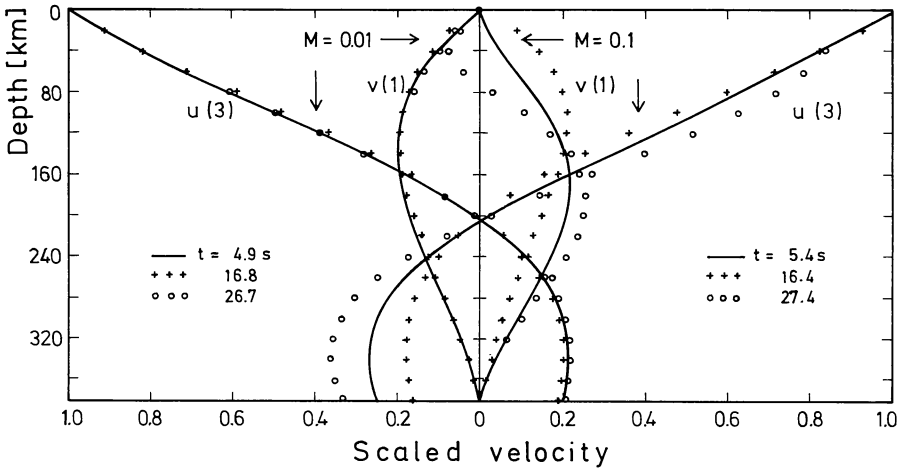

Fig. 4a and b. Acoustic standing waves with vertical Mach numbers $M = 0.01$ and 0.1. **a** Pressure on the axis $p(1)$ and the cylinder boundary $p(6)$. **b** Vertical velocity on the axis $v(1)$ and horizontal velocity 40 km from the axis $u(3)$. All curves are normalized to maximum values of $p(1)$ and $u(3)$ of unity, at intervals of about 1/2 period ($P = 21.95$ s)

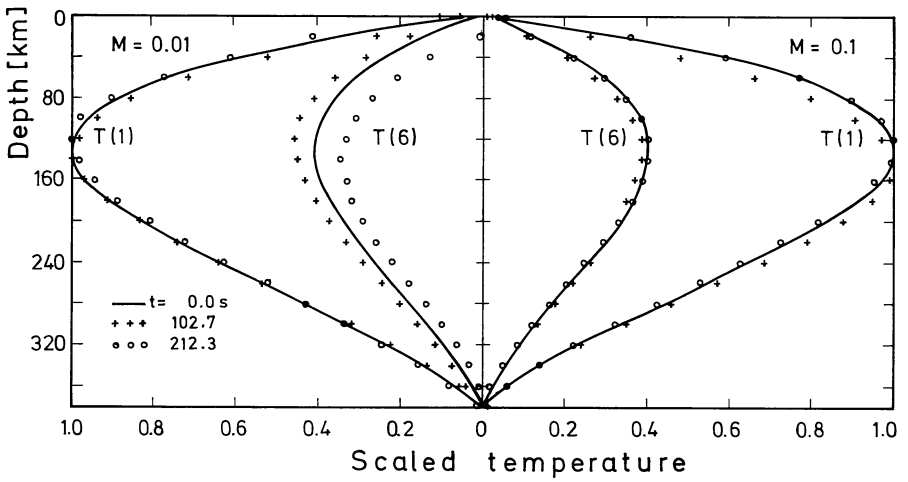

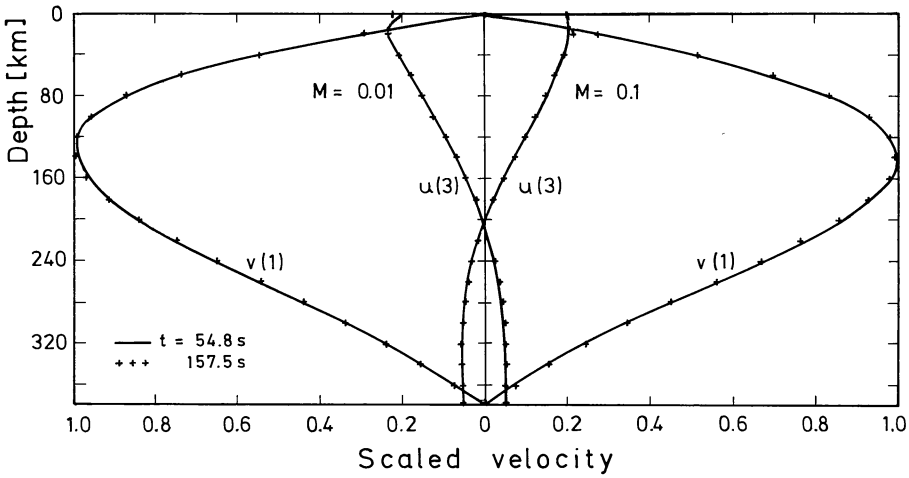

Fig. 5a and b. Internal gravity waves with vertical Mach numbers $M = 0.01$ and 0.1. **a** Temperature on the axis $T(1)$ and the cylinder boundary $T(6)$. **b** Vertical velocity on the axis $v(1)$ and horizontal velocity 40 km from the axis $u(3)$. All curves are normalized to maximum values of $T(1)$ and $v(1)$ of unity, at intervals of about 1/2 period ($P = 210.1$ s)

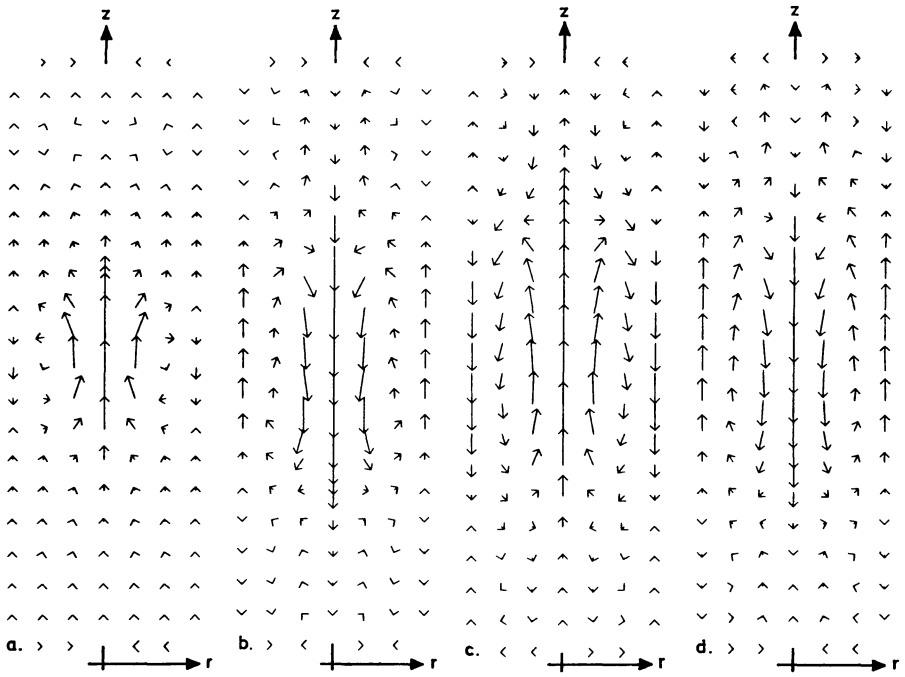

Fig. 6a–d. Velocity field of an oscillating gas bubble. **a** Time step $K=33$, time $t=45.2$ s. **b** $K=119$, $t=163.1$ s. **c** $K=198$, $t=271.2$ s. **d** $K=267$, $t=365.8$ s. The phases displayed show maximum vertical velocity

b) Brunt-Väisälä oscillations

Another test of the proposed code is the calculation of the Brunt-Väisälä oscillation of an adiabatic gas bubble in an isothermal gravitational atmosphere. Such an oscillation is stable and has been discussed e.g. by Hines (1960). For our test an atmosphere with a temperature of 5000 K and solar gravity was chosen. We have adopted 20 vertical and 4 horizontal points with intervals of 20 km in either direction. The gas bubble was centered on the axis at depth point 10 and extended 3 grid points in every direction in which the temperature perturbation was assumed to decrease to zero from a maximum value of 250 K. In applying the temperature perturbation to the initial atmosphere the pressure was assumed to be unchanged (isopressure bubble). Figure 6 shows the velocity field of the oscillating gas bubble at indicated time steps (of 1.37 s each). The time steps displayed are phases of maximum upward or downward vertical velocity. Since this imposed perturbation is not an eigenmode of the rigidly enclosed system, it is seen that, through gravity wave action, the oscillatory motion of the gas bubble spreads over the entire volume with an associated reduction of the magnitude of the vertical velocity. A third upward velocity maximum occurs at time step 350. From consecutive maxima of the same phase we derive oscillation periods. For the upward maxima we find periods decreasing from 226 s to 208 s while the downward maxima give a period of 203 s. This agrees nicely with a Brunt-Väisälä period $P_{BV}=2\pi a/\sqrt{\gamma-1}\,g=205$ s for the atmosphere. The computation time for 400 time steps on the IBM 370-168 was 3.5 min.

5. Discussion and conclusion

We have described above a formulation of the nonlinear dynamics applicable in stellar atmospheres. This code has very distinct advantages on both physical and numerical grounds.

Because of the highly accurate two-dimensional spline interpolation, the solution can be well represented with only few grid points. This has already been found in our one-dimensional work (cf. Hammer and Ulmschneider, 1978), and for the present two-dimensional application contributes greatly to the reduction of computation time.

Furthermore, if the boundaries are kept fixed, the grid points can be readily adjusted from time step to time step in order to improve resolution as required. In principle, this method, as all characteristic methods, is not limited by the Courant condition since the domain of dependence is sought explicitly by our interpolation in the old time level. However, to greatly increase the time step beyond the Courant results in significant loss of accuracy.

At present the code does neither handle radiation nor allows treatment of shocks. However, two-dimensional radiation transport can be incorporated without great difficulty as a simple generalization of our one-dimensional method. In many situations, e.g. in granular flow, it may even suffice to consider only vertical transfer of radiation for which the one-dimensional procedure can be adopted without change.

Considerable programming effort, however, is necessary for the treatment of shocks, although it also is only a straightforward extension of our one-dimensional procedure. In subsequent work we will present applications of the present method in which both radiation and shocks are handled.

In principle, the great advantage of our present method is that it lends itself to an explicit treatment of shock discontinuities. The shock structure can be resolved and one does not need to pay the price of including many grid points and artificial viscosity as in finite difference schemes. Our one-dimensional work clearly shows that, once the programming logic has been successfully dealt with, the shock points can be treated about as speedily as any regular grid points.

Of course, the code has its limitations which require brief discussion. The most obvious restriction is the inclusion of only two spatial dimensions. The only three-dimensional numerical

investigation of a stellar model is that of Nordlund (1982). The price paid for the greater number of spatial dimensions is the increased length of time required to compute each time step. In three dimensions it is economic to treat only the anelastic problem which filters out sound waves and makes a short time step unnecessary. As yet, modelling with full compressibility effects are necessarily two-dimensional. Cloutman (1979) justified this restriction in his implicit numerical formulation by appeal to the success of two-dimensional models in predicting the time behaviour of terrestrial fireballs. The mean flow in granules, as in fireballs, is essentially axisymmetric. This property is preserved in the code presented above, which is thus closer to the prototype than that of Cloutman which employed Cartesian geometry.

The second obvious failing is the neglect of viscosity. Molecular viscosity is dynamically unimportant in stellar atmospheres where the Prandtl number is only 10^{-9}, but it must be considered in the global energy balance. The highly turbulent character of the convective systems that result in stellar envelopes makes it impossible to compute the motions down to the viscous scale. Only the large-scale mean motion can be treated, and these feel the effects of viscosity indirectly through the loss of kinetic energy into a turbulent cascade that proceeds beyond the spatial resolution of the simulation. This transfer is only possible in a truly three-dimensional hydrodynamic treatment, so it must be modelled, more or less satisfactorily, by the introduction of a turbulent viscosity in some form in two-dimensional codes, or it must be neglected entirely. We have adopted the second approach.

This procedure is doubtful if we were to attempt to model the dynamics of the convection zone itself. It was adopted by Deupree (1976) in a study of nonlinear convection in shallow stellar envelopes. The energy balance is not correctly treated and Deupree's models failed to reach a steady-state.

But this is not critical for our purposes. Any convective motion can be initiated by introducing a suitable perturbation into a layer in unstable equilibrium with a superadiabatic stratification. We can then expect that the dynamics will provide "at least semi-quantitative agreement with granule observation", to quote Cloutman (1979). The rise of the bubble can be followed into a stably stratified atmosphere. The fate of the sinking material displaced by the rising bubble is decided somewhat arbitrarily by imposing a rigid lower boundary condition. But this has little influence on the region of primary interest. The atmospheric dynamics are correctly treated and describe fully the coupling of the convective field, which must at this stage be imposed, to the acoustic and internal wave fields.

Acknowledgements. We want to acknowledge generous support from the Deutsche Forschungsgemeinschaft.

References

Butler, D.S.: 1960, *Proc. Roy. Soc. London* **255**A, 232
Chiu, Y.T.: 1970, *Physics of Fluids* **13**, 2950
Chow, T.: 1973, *J. Comp. Phys.* **12**, 153
Chu, C.W.: 1967, AIAA *Journal* **5**, 493
Cline, M.C., Hoffman, J.D.: 1972, AIAA *Journal* **10**, 1452
Cline, M.C., Hoffman, J.D.: 1973, *J. Comp. Phys.* **12**, 1
Cloutman, L.D.: 1979, *Astrophys. J.* **227**, 614
Courant, R., Friedrichs, K.: 1948, Supersonic Flow and Shock Waves, Interscience, New York
Courant, R., Hilbert, D.: 1962, Methods of Mathematical Physics, Vol. II, Interscience, New York
Deupree, R.G.: 1976, *Astrophys. J.* **205**, 286
Elliot, L.A.: 1962, *Proc. Roy. Soc. London* **267**A, 558
Falle, S.: 1976, *Observatory* **96**, 175
Finkleman, D.: 1969, AIAA *Journal* **7**, 1602
Finkleman, D., Baron, J.R.: 1970, AIAA *Journal* **8**, 87
Gough, D.O.: 1969, *J. Atmos. Sci.* **26**, 448
Hammer, R., Ulmschneider, P.: 1978, *Astron. Astrophys.* **65**, 273
Hedstrom, G.W.: 1979, *J. Comp. Phys.* **30**, 222
Hines, C.O.: 1960, *Canadian J. Phys.* **38**, 1441
Hoskin, N.E.: 1964, *Meth. Comp. Phys.* **3**, 265
Jordan, S.: 1982, The Sun as a Star, CNRS Paris/NASA Washington
Kalkofen, W., Ulmschneider, P.: 1977, *Astron. Astrophys.* **57**, 193
Kot, C.A.: 1973, *Proc. Third Intern. Conf. Num. Methods Fluid Mechanics*, Lecture Notes Phys. **18**, Springer, Heidelberg, p. 130
Lax, P.D.: 1954, *Comm. Pure Appl. Math.* **7**, 159
Lister, M.: 1960, Mathematical Methods for Digital Computers, Vol. I, eds. A Ralston, H. Wilf, Wiley, New York
McCormack, R.W.: 1976a, NASA TM X-73, 129
McCormack, R.W.: 1976b, in *Proc. Fifth Intern. Conf. Num. Meth. Fluid Dyn.*, Lecture Notes Phys. **59**, Springer, Heidelberg, p. 307
Mihalas, B.M., Toomre, J.: 1981, *Astrophys. J.* **249**, 349
Moretti, G.: 1975, in *Proc. Fourth Intern. Conf. Num. Methods Fluid Dynamics*, Lecture Notes Phys. **35**, Springer, Heidelberg, p. 287
von Neumann, J., Richtmyer, R.D.: 1950, *J. Appl. Phys.* **21**, 232
Nordlund, A.: 1982, *Astron. Astrophys.* **107**, 1
Ransom, V.H.: 1970, PhD Thesis, Purdue Univ.
Richardson, D.J.: 1964, *Meth. Comp. Phys.* **3**, 295
Richtmyer, R.D.: 1973, in *Proc. Third Intern. Conf. Num. Methods Fluid Mechanics*, Lecture Notes Phys. **18**, Springer, Heidelberg, p.72
Sachdev, L., Prasad, P.: 1966, *Phys. Soc. Japan*, **21**, 2715
Sauerwein, H.: 1964, Ph. D. Thesis, MIT
Sauerwein, H.: 1966, *J. Fluid Mech.* **25**, 17
Sauerwein, H.: 1967, *J. Comp. Phys.*, **1**, 406
Shin, Y.W., Valentin, R.A.: 1976, *J. Comp. Phys.* **20**, 220
Spiegel, E.A., Veronis, G.: 1960, *Astrophys. J.* **131**, 442
Späth, H.: 1973, Spline-Algorithmen zur Konstruktion glatter Kurven und Flächen, Oldenburg, München, p. 111
Stefanik, R.P.: 1973, Ph. D. Thesis, Harvard Univ.
Stix, M.: 1969, Ph. D. Thesis, Univ. Munich
Stein, R.F.: 1968, *Astrophys. J.* **154**, 297
Ulmschneider, P., Kalkofen, W., Nowak, T., Bohn, U.: 1977, *Astron. Astrophys.* **54**, 61
Ulmschneider, P., Schmitz, F., Kalkofen, W., Bohn, H.U.: 1978, *Astron. Astrophys.* **70**, 487
Weiss, N.O.: 1977, in *Problems of Stellar Convection*, Lecture Notes Phys. **71**, Springer, Heidelberg, p. 142
Zahn, J.P.: 1979, in *Stellar Turbulence*, *Proc.* IAU *Coll.* **51**, Lecture Notes Phys. **114**, Springer, Heidelberg, p. 1